

# Surfaces of mixed formulation solder alloys at melting

M. J. Bozack,<sup>a)</sup> J. C. Suhling, Y. Zhang, Z. Cai, and P. Lall

Center for Advanced Vehicle and Extreme Environment Electronics (CAVE3), Auburn University, Auburn, Alabama 36849

(Received 19 January 2011; accepted 11 April 2011; published 24 May 2011)

Mixed formulation solder alloys refer to specific combinations of Sn-37Pb and SAC305 (96.5Sn–3.0Ag–0.5Cu). They present a solution for the interim period before Pb-free electronic assemblies are universally accepted. In this work, the surfaces of mixed formulation solder alloys have been studied by *in situ* and real-time Auger electron spectroscopy as a function of temperature as the alloys are raised above the melting point. With increasing temperature, there is a growing fraction of low-level, bulk contaminants that segregate to the alloy surfaces. In particular, the amount of surface C is nearly ~50–60 at. % C at the melting point. The segregating impurities inhibit solderability by providing a blocking layer to reaction between the alloy and substrate. A similar phenomenon has been observed over a wide range of (SAC and non-SAC) alloys synthesized by a variety of techniques. That solder alloy surfaces at melting have a radically different composition from the bulk uncovers a key variable that helps to explain the wide variability in contact angles reported in previous studies of wetting and adhesion. © 2011 American Vacuum Society. [DOI: 10.1116/1.3584821]

## I. INTRODUCTION

The wetting of solid surfaces by liquid metal alloys occurs in many technological processes and constitutes an integral part of the structure of materials. Processes of liquid phase sintering, detergency, adhesion, wear, catalysis, impregnation of porous materials by liquid binders, crystal growth from the melt, and solderability are largely determined by the ability of a liquid alloy to wet and spread evenly over a solid substrate. Elucidation of the fundamental thermochemical mechanisms operating at the contacting boundaries in a system between liquids and solids is therefore of great importance.

Despite the importance of the interfacial surface chemistry in wetting reactions, there have been comparatively few studies of liquid surfaces using surface analytical techniques, largely due to the risk involved when heating materials to melting inside expensive ultrahigh vacuum systems. Hardy and Fine<sup>1</sup> noted, in 1982, for example, that they were aware of only two previous applications<sup>2,3</sup> of Auger spectroscopy to the study of liquid surfaces. In light of the limited amount of studies of the liquid–gas interface, this report presents some of the first conclusions from studies of the surface behavior of new, mixed-formulation, and SAC-based solder alloys.

Mixed-formulation solders are combinations of Sn-37Pb and SAC305 (96.5Sn–3.0Ag–0.5Cu) in specific mole fractions. The resulting solder joints are quaternary alloys of Sn, Ag, Cu, and Pb. Current interest in mixed alloys is due to the mandated shift from eutectic Sn-37Pb solder to emerging Pb-free solders in electronics applications. They represent a solution for the interim period before Pb-free assemblies are uniformly accepted. There are two varieties of mixed solder assemblies. When conventional Sn-Pb solder paste is mixed

with components with SAC solder balls or component leads with SAC finishes, the process is coined as a “backward compatible” process (see Fig. 1). When SAC pastes and processes are mixed with components with Sn-Pb solder balls or components/PCBs with Sn-37Pb surface finishes, the process is referred to as a “forward compatible” process.

To date, research on mixed formulation alloys has focused on the reliability and process variables for mixed-formulation solders.<sup>4–8</sup> There has been comparatively little work on the wetting behavior, especially using surface analytical techniques. In the present effort, we report experiments using Auger electron spectroscopy (AES), which are designed to study the surfaces of mixed formulation solder alloys under real-time, *in situ* conditions as the alloys are heated through the melting point. This is a primary factor in wetting since the condition of the molten surface at and above the melting point affects the liquid–solid and liquid–gas interfacial tensions and consequent ability of the alloy to react with the joining solid surface. We find that the composition of the molten solder alloy surface is *radically different* from the surface composition at room temperature, with a direct and deleterious effect on wetting.

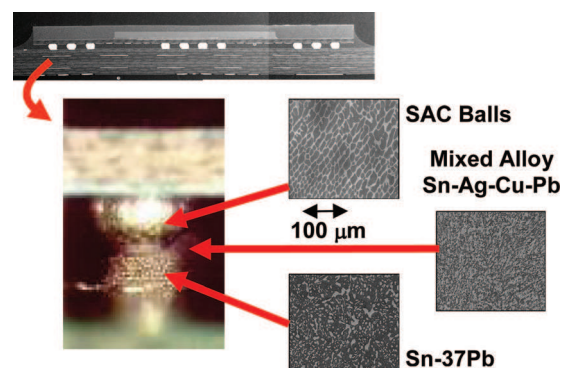


FIG. 1. (Color online) Backward compatible mixed assembly.

<sup>a)</sup>Electronic mail: bozack@physics.auburn.edu

## II. MATERIALS AND EXPERIMENTAL PROCEDURES

The mixed formulation alloys were seven different mixture ratios of Sn-37Pb and SAC305. Two were the pure solder alloys (Sn-37Pb and SAC305) and five were mixtures determined by the weight percentages of the two alloys. We refer to each mixed alloy with the nomenclature MIX A-B, where A and B are the weight percentages of the two alloys: e.g., MIX 30-70 is a solder mixture of 30 wt.% Sn-37Pb and 70 wt.% SAC305. The chemical compositions of the mixed alloys are given in Table I.

The solder specimens were prepared by drawing the mixed alloys into high precision rectangular cross section glass tubes using vacuum suction. One end of the glass tube is inserted into the molten solder and suction is applied to the other end by a rubber tube connected to the house vacuum system. The suction forces are controlled through a regulator on the vacuum line so that only a desired amount of solder is drawn into the tube. The tubes are then cooled by water quenching to yield a fine microstructure (Fig. 2). The specimen preparation hardware is shown in Fig. 3. The measured melting points and pasty range of the resulting mixed formulation solders are shown in Fig. 4.

The wetting substrate was aluminum metal covered with a native aluminum oxide, verified by x-ray photoelectron spectroscopy (XPS). This selection was made because aluminum oxide has an extremely large and negative Gibbs free energy of formation,<sup>9</sup> which produces a high wetting contact angle for most materials due to the high chemical stability and lack of chemical reaction and interdiffusion. High rates of chemical reaction and low contact angles would unnecessarily confound the data interpretation due to diffusion of substrate elements into the alloy. The experimental design sought to completely isolate the wetting system from any outside elemental influences.

In the composition versus temperature experiment, the mixed alloy was laid atop the aluminum oxide substrate and introduced into the ultrahigh vacuum system. The alloy fragment was rectangular in shape ( $\sim 2 \times 3 \times 1$  mm in height) and held in contact with the substrate by gravity without solder flux. After the base pressure was achieved, the alloy surface was sputter cleaned with argon and then heated in 50 °C increments (1 °C/s rate) until the alloy melted. In the earliest experiments, the system base pressure of  $1 \times 10^{-10}$  Torr was maintained throughout a series of preliminary studies of the

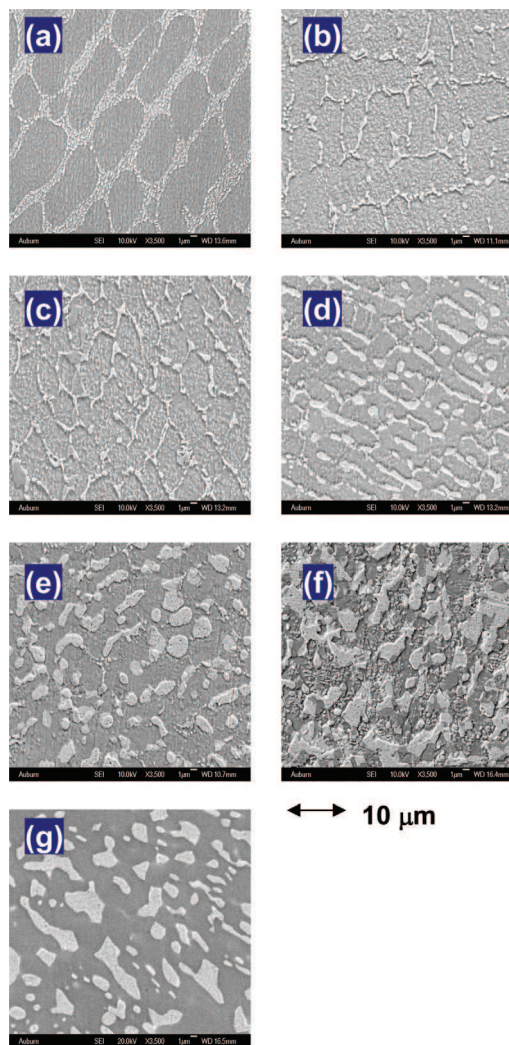


FIG. 2. (Color online) Scanning electron microscopy (3500 $\times$ ) photographs of the microstructures of quenched, as-cast mixed formulation solder alloys (a) SAC305, (b) MIX 10-90, (c) MIX 30-70, (d) MIX 50-50, (e) MIX 70-30, (f) MIX 90-10, and (g) Sn-37Pb.

alloy surfaces. Later work showed higher system pressures to have little effect on the contact properties and this requirement was relaxed to the base pressure of the system ( $5 \times 10^{-9}$  Torr) without bakeout. Alloy heating was accomplished inside the vacuum system by a high resistivity heater element inserted into the bottom of the stainless steel sample mount holding the aluminum oxide and alloy. The approximate temperature of the alloy was indicated by a thermocouple built into the heater element. The melting point was easily verified by SEM observations of morphological changes in the alloy at melting (the XSAM 800 is a scanning Auger system) and by the pressure burst at melting due to release of trapped gases in the alloy. The Auger beam was positioned near the top of the alloy fragment, although the beam position had to be moved occasionally as the alloy changed shape from rectangular to spherical during melting. The contact angle of mixed formulation and SAC alloys on aluminum oxide changed from 0° before heating to  $\sim 180^\circ$  after melting. The adhesive forces were so low that, on a few rare occasions, the spherical molten alloy droplet rolled off

TABLE I. Composition of mixed formulation alloys (wt.%).

Solder type	Mixing proportion (%)				
	(Sn-Pb:SAC305)	Sn	Pb	Ag	Cu
SAC305	0 (0:100)	96.5	0	3	0.5
MIX 10-90	10 (10:90)	93.15	3.7	2.7	0.45
MIX 30-70	30 (30:70)	86.45	11.1	2.1	0.35
MIX 50-50	50 (50:50)	79.75	18.5	1.5	0.25
MIX 70-30	70 (70:30)	73.05	25.9	0.9	0.15
MIX 90-10	90 (90:10)	66.35	33.3	0.3	0.05
Sn-37Pb	100 (100:0)	63	37	0	0

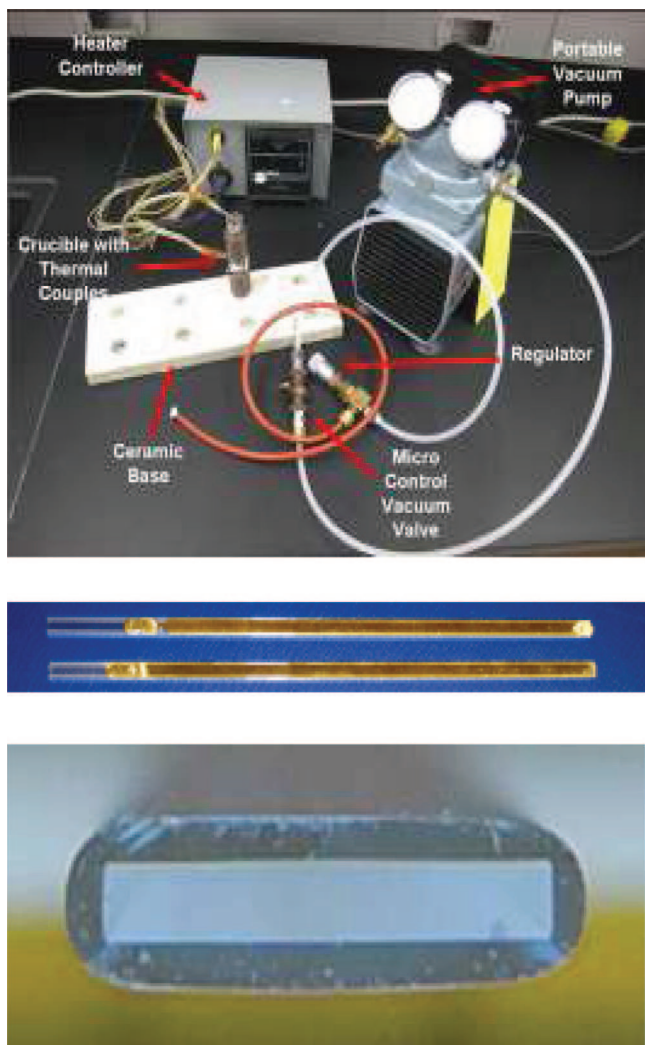


FIG. 3. (Color online) (Top) Mixed formulation specimen preparation hardware; (middle) mixed alloy within glass tubes after vacuum suction; (bottom) resultant alloy cross-section.

the aluminum oxide substrate and into the bottom of the vacuum chamber. Each Auger spectra required about 20 min to acquire during which time the alloy was maintained at the target temperature.

The surface system was a load-locked Kratos XSAM 800 multitechnique surface analysis instrument shown in Fig. 5. The unbaked base pressure of this ion- and turbo-pumped system is  $5 \times 10^{-9}$  Torr as read on an uncalibrated nude ion gauge. The electron energy analyzer for the AES/XPS portion of the system is a 127 mm radius double focusing concentric hemispherical energy analyzer equipped with an aberration compensated input lens. AES spectra were recorded in the fixed retard ratio mode with a retard ratio of 10. Such a retard ratio represents a compromise between sensitivity and resolution and is appropriate for acquisition of survey spectra. The AES energy axis was calibrated by setting the Cu(LMM) line to 914.4 eV referenced to the Fermi level.

To clean the starting alloy surfaces of adsorbed gases, light  $\text{Ar}^+$  ion sputter cleaning was accomplished by a differentially pumped Kratos Minibeam I plasma discharge ion

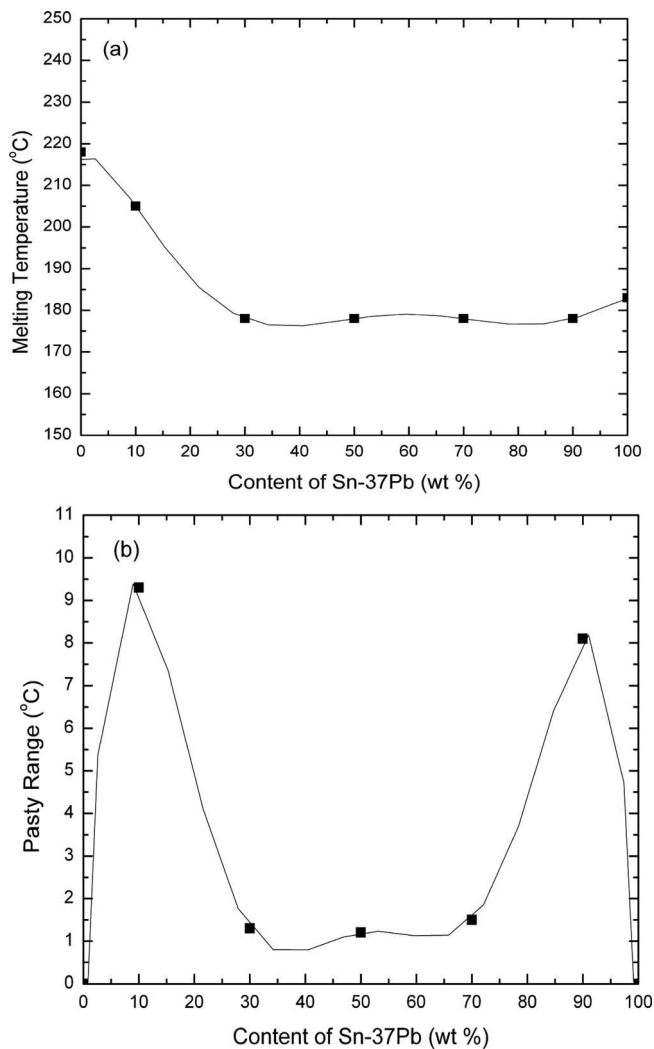


FIG. 4. Measured physical properties of mixed formulation solder alloys: (a) melting temperature and (b) pasty range.

source with rastering and focusing capabilities. A variable scan voltage provides a high frequency scan mode, which yields a sputtered area of  $1 \text{ cm}^2$  at the specimen position with a sputter rate of  $\sim 25 \text{ \AA}/\text{min}$  measured on a standard  $\text{SiO}_2$  film. Auger spectra were taken on the alloy surface from a focused beam spot ( $\sim 0.1 \text{ mm}$ ) at a position near the center of the sputtered area. The angle of incidence of the ion beam with respect to the surface normal was  $55^\circ$ . All Auger spectra were recorded at 3.0 keV beam energy and  $0.7 \mu\text{A}$  primary beam current, measured with applied +90 V bias. The detection system of the XSAM 800 consists of a single channel multiplier and a fast response head amplifier. Detector output modes include direct pulse counting and current detection with voltage to frequency (V-F) conversion. Due to the large exciting currents used, all spectra were recorded in V-F detection mode.

The raw Auger data was collected as  $E N(E)$  by acquiring the spectrum of electrons emitted from the surface from an energy 50–600 eV, with a starting energy of 50 eV to avoid collecting data from the intense, broad secondary electron peak occurring in this energy region. For most mixed formulation and SAC alloys, the atomic fraction of Ag and Cu is

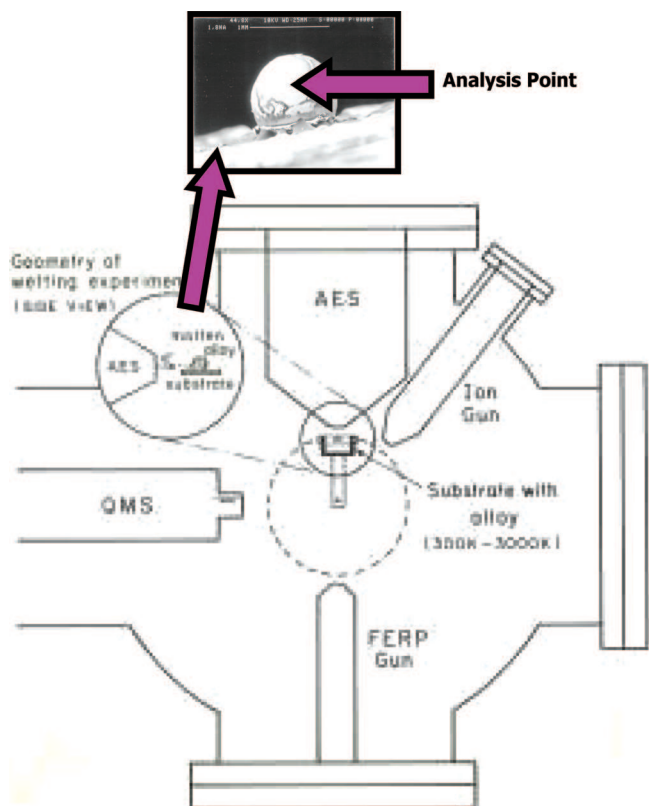


FIG. 5. (Color online) Schematic diagram of the ultrahigh vacuum section of the surface analytical system used for *in situ*, real-time AES liquid surface studies of mixed formulation alloys.

so small that the Auger spectrum is dominated by the triplet Sn(MNN) peaks from 320 to 440 eV and the low energy Pb feature at 94 eV. The low weight percent component Ag, having a principal (MNN) peak at 356 eV, and Cu, with a primary Cu(LMM) peak at 920 eV, are barely visible. The Savitzky-Golay<sup>10</sup> routine was employed to smooth the data and calculate the derivative Auger spectrum. Surface elemental compositions were determined by standard relative Auger sensitivity factors<sup>11</sup> supplied by the instrument manufacturer. It is the trend in relative Auger peak-to-peak heights during heating that is significant rather than the accuracy ( $\sim 10$ – $20\%$ ) of the surface composition numbers. It is well known that stoichiometric calculations in AES are problematic due to complexities inherent in the production, transmission, and detection of Auger electrons. While we report here on mixed formulation solder alloys, similar experiments in our laboratory on commercial SAC-series (SAC105, 205, 305, and 405) compositions and special solder compositions gave similar results.

### III. RESULTS

#### A. Alloy surface composition versus temperature

The surface composition as a function of temperature for MIX 90-10 wetted to aluminum oxide is shown in Fig. 6. The result is representative for all mixed formulation series alloys (MIX 10-90, 30-70, 50-50, 70-30, and 90-10). A sloping increase in the fraction of surface C and O (with an accompa-

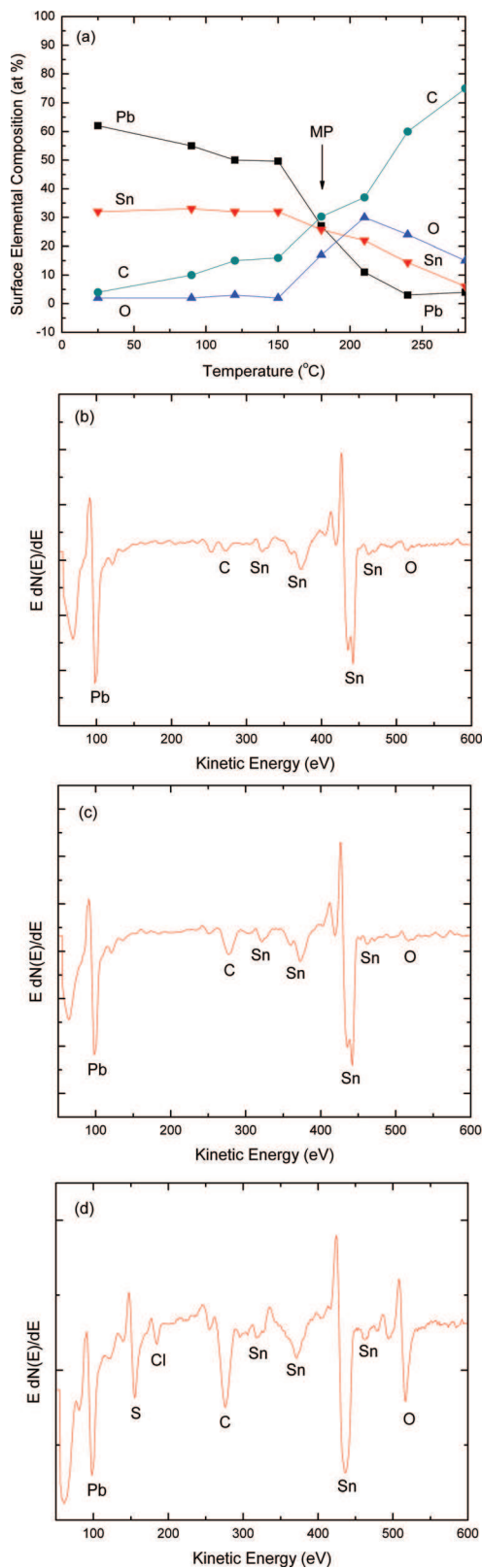


FIG. 6. (Color online) (a) Auger surface elemental composition of MIX 90-10 alloy vs temperature; individual AES survey spectra for three temperatures: (b) RT, (c) 150 °C, and (d) MP.

nying decrease in Sn) is typically observed with increasing temperature, in some cases from  $\sim 0$  at.% C at room temperature to  $\sim 50$ – $70$  at.% C at the alloy melting temperature. The increase begins before reaching the melting point. Figure 6(a)

plots the trend with temperature and Fig. 6(b) displays individual survey AES spectra at three of the temperatures. Clearly, the most distinctive feature during annealing is the dramatic growth of the C(KLL) Auger peak at 272 eV. Small concentrations of other low-level alloy impurities such as S, Ca, and P are also frequently observed, particularly at the melting point. *In situ* optical and electron microscopy observations of the resultant molten, poorly wetted droplet frequently showed evidence of second phase material floating on the surface of the liquid alloy. Cooling the alloy back to room temperature did not reverse the surface composition. Figures 7 and 8 show similar trends for the SAC305 and Sn-37Pb used to mix the alloys.

Repeat measurements of composition versus temperature on alloy fragments cut from the same bar of as-cast solder revealed statistical variations when measuring the surface properties of liquid metal alloys. The elemental trends seen in Figs. 6–8 are nearly always observed but, as the electron micrographs in Figs. 5 and 9 of poorly wetted droplets show, the alloy surfaces are inhomogeneous due to the shell of segregated impurities (primarily C). Real-time observations of the molten droplets by low power zoom optical microscopy during heating in the vacuum system revealed that it is possible for parts of the C surface crust to dynamically move during the course of the measurements, bringing different portions under the AES beam, resulting in compositional variations over repeated experiments. Figure 9 shows an example of the room temperature segregated C shell appearance in a low-power optical (white light) microscopy after wetting a mixed formulation solder alloy MIX 10-90 to a Ni-Au board finish (no flux applied), showing an area of the alloy surface with  $\sim 100\%$  surface segregated C content (poor wetting and high contact angle) and low C content (good wetting and low contact angle). The AES spectra were recorded directly after wetting in the surface analysis system (no breaking of vacuum).

## B. From whence the surface carbon

Using an inert wetting substrate and the ability to sputter clean the alloy surface of adsorbed gases before heating proved to be essential features of the experiment. Since the alloy was isolated from outside sources of carbon and other elemental species, the material observed at the alloy surfaces during heating could only originate from the alloy itself in the form of low-level surface segregated impurities. Similar behavior has been found when SAC alloys are wetted (without flux) to more reactive common electronic board finishes (Ni-Au, Pd-Ni, Ag-Cu, HASL, etc.).<sup>12</sup> It is generally the case (shown in Fig. 9) that in regions of the alloy where sluggish and/or nonexistent wetting/spreading occurs, high concentrations of surface carbon are present.

There are four lines of evidence for surface segregation of low-level impurities in the liquid alloys. First, there is direct experimental proof of large relative concentrations of low-level impurities at heated alloy surfaces, sometimes as high as  $\sim 100$  at.% in the case of C. When wetting to inert nonmetallic solids, the segregated materials act to inhibit wetting. On reactive board finishes such as Ni-Au and Ag-Cu,

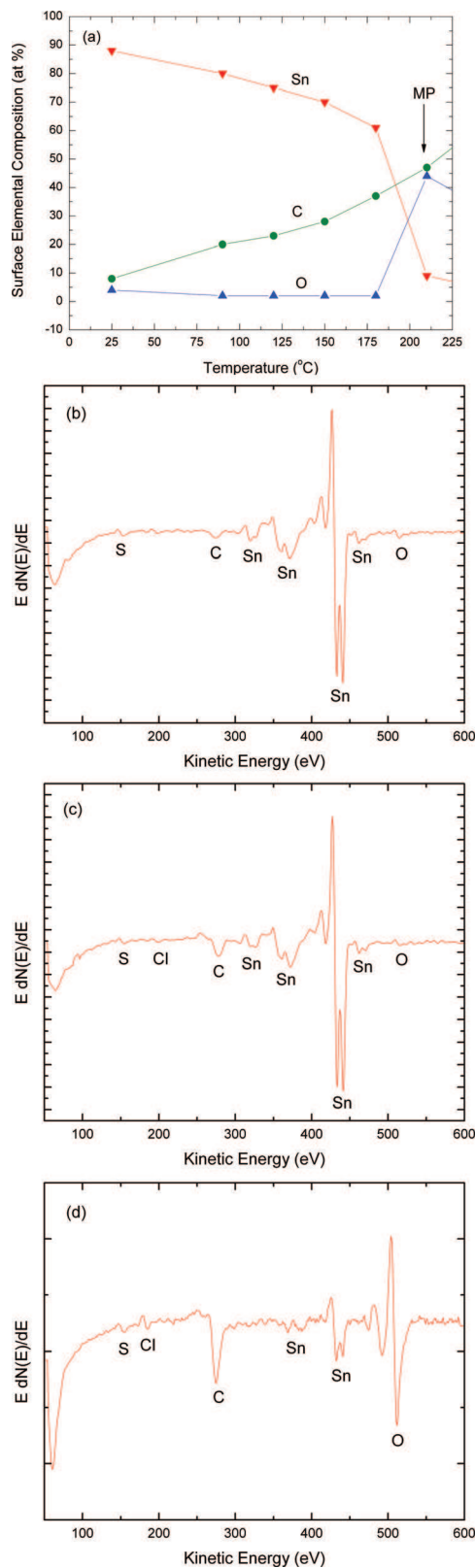


FIG. 7. (Color online) (a) Auger surface elemental composition of SAC305 alloy vs temperature; individual AES survey spectra for three temperatures: (b) RT, (c) 150 °C, and (d) MP.

wetting occurs with small contact angles despite the presence of the surface impurities. This is due to the strong chemical reaction of many metallic substrates, which are known to readily diffuse into the alloy.

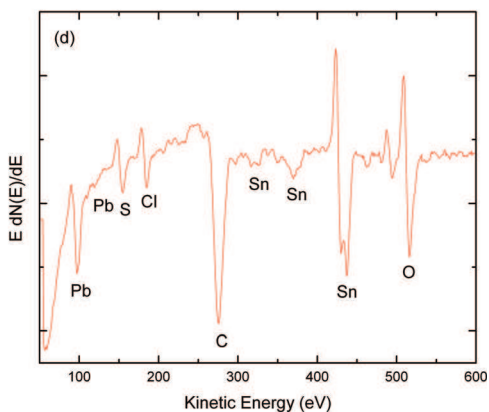
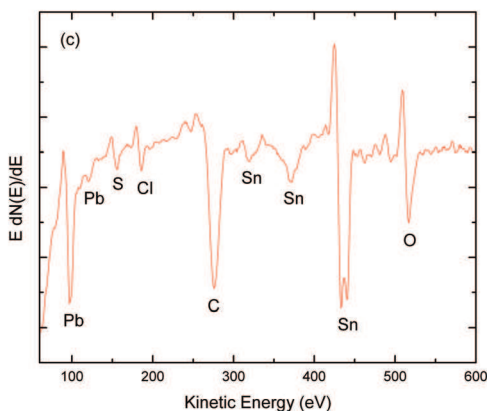
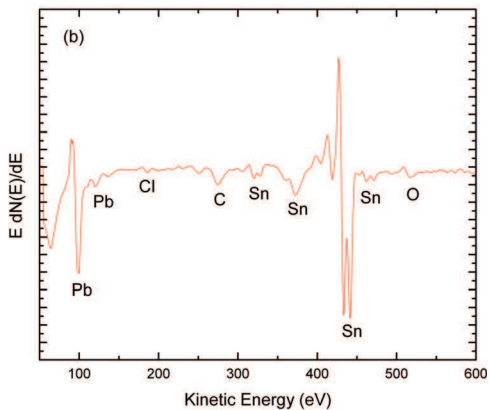
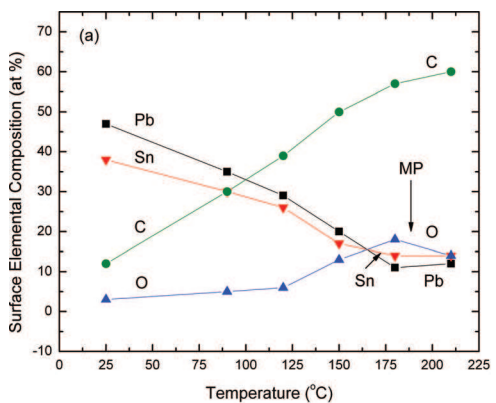


FIG. 8. (Color online) (a) Auger surface elemental composition of Sn-37Pb alloy vs temperature; individual AES survey spectra for three temperatures: (b) RT, (c) 150° C, and (d) MP.

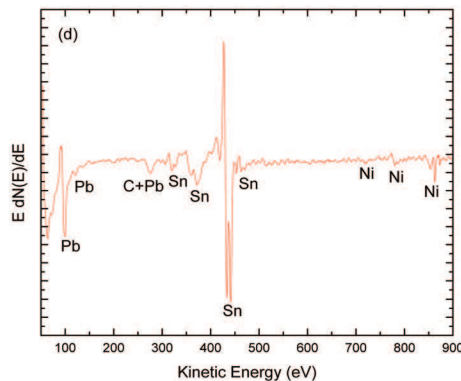
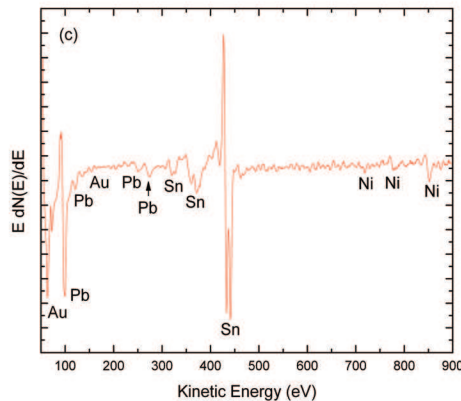
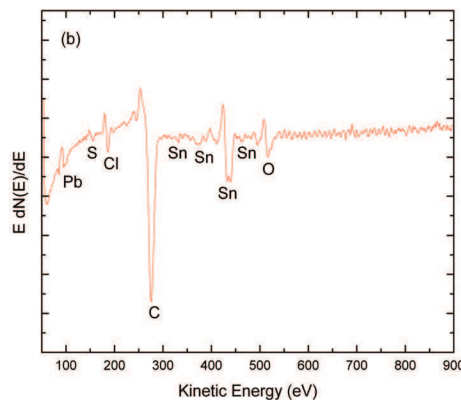
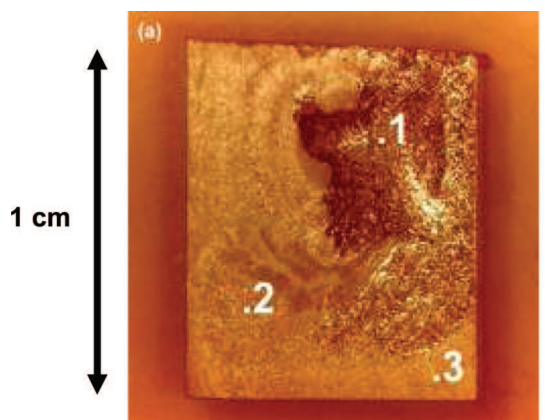


FIG. 9. (Color online) Effects of impurity segregation on wetting. (a) Optical photograph of MIX 10-90 wetted to Ni-Au (no flux applied) showing areas of the alloy surface with (b) ~100% surface segregated C content (poor wetting and high contact angle, position 1) and (c), (d) low C content (good wetting and low contact angle, positions 2 and 3). The AES spectra were recorded directly after wetting in the surface analysis system.

Second, sanity check calculations of surface enrichment show that it is possible for the high concentrations of carbon observed at the molten surfaces to originate from surface-segregated material. Assuming a typical level of bulk C alloy contamination just below the detection limit of energy dispersive x-ray (EDX) spectroscopy ( $\sim 0.02$  wt.%) and presuming the entire weight percent of carbon segregates to the surface of a spherical droplet of SAC alloy whose radius is 0.5 mm, the thickness of the carbon shell formed is  $T = 3.17 \times 10^{-6} \cdot (\rho_{SAC}/\rho_C)\text{cm} \approx 100 \text{ nm}$  where  $T$  is the shell thickness in nanometers and  $\rho_{SAC}$  and  $\rho_C$  are the densities of a typical SAC alloy and graphite, respectively. We have assumed the density of graphite to be  $2.0 \text{ g/cm}^3$  and the density of SAC 405 as  $7.4 \text{ g/cm}^3$  from values given in the literature.<sup>13</sup> Bulk emission spectroscopic analysis from a variety of solder alloys shows that such levels of carbon contamination are the rule rather than the exception for commercial alloys. To verify the order of magnitude calculation, we measured the thickness of the surface carbon shell formed on several poorly wetted spheres of SAC and Sn-37Pb alloy by Auger depth profiling. In most cases, the measured carbon shell was  $\sim 800\text{--}1200 \text{ \AA}$  in thickness.

Third, metallographic examinations of the interior and near-surface microstructure of poorly wetted droplets after cooling to room temperature show drastic differences. A typical case is shown in Fig. 9, which is an optical microscope photograph of a quenched MIX 10-90 alloy wetted to a Ni-Au board finish. It is clear that the segregated shell remnant at position 1 is composed of second phase material. Similar examinations of cross-sectional slices through the wetted alloy showed no evidence of second-phase carbon in the droplet interior. In early studies of this issue using high-temperature Ni-B alloys, we often observed hexagonal graphite formation on the surfaces of the quenched boride alloys but not in the alloy interior.<sup>14</sup>

Fourth, the spectroscopic composition of alloy material in the interior of poorly wetted droplets is free of impurities, at least to the detection limit ( $\sim 0.1$  wt.% or  $\sim 20\text{--}200$  ppm.)<sup>15</sup> of Auger and EDX spectroscopy. It is possible to fracture the carbon shell surrounding poorly wetted droplets by thermal (rapid temperature excursions) or mechanical (stylus puncture) means. The efflux of alloy material consists of pure alloy components that are able to wet and spread over many common board finishes without the aid of flux. With highly reactive substrates such as Ni-Au, the wetting occurs despite the surface C shell, which is left behind as an inert remnant of carbon (cf. Fig. 9). The fact that those impurities are found on the surface of the droplet but not in the interior is evidence for impurity surface segregation.

#### IV. DISCUSSION

The primary goal of this work was to determine what a solid substrate sees during wetting of molten mixed formulation solder alloys. Since the soldering process involves heating the solder to a temperature greater than the alloy melting point, the substrate sees the liquid surface above the melting point, not the solid alloy surface at room temperature. If the

solid and liquid solder surfaces are elementally different, presumptions made by flux chemists about what surface species exist on solder alloy surfaces will result in inefficient flux formulations. It has been shown that wetting in many solder alloy systems is strongly influenced by surface segregation of low-level bulk impurities, which arise from the alloy bulk. The segregated impurities form a barrier, which inhibits reactions between alloys and substrates and results in poor contact angles. There are at least three possible solutions to this problem.

The first solution is to eliminate the bulk alloy impurities by employing ultrapure starting materials and strict control of the alloy synthesis process. This is not easy to accomplish in a cost-effective way. The impurity level necessary to prevent build-up of a few monolayers of segregated material is in the parts per million range and would require extraordinary processing conditions. A typical arc melting apparatus, for example, operates under an inert gas atmosphere with a pressure of at least several Torr with no provision for evacuation to high vacuum. Even assuming perfectly pure starting elemental materials, common impurities such as nitrogen, oxygen, and carbon can readily become incorporated into the alloy bulk during synthesis. It is likely that surface segregation of low-level bulk impurities is a ubiquitous phenomenon spanning a wide variety of alloys and alloy synthesis techniques. We have now observed it in boride alloys manufactured by the arc melting technique, arsenide alloys manufactured by the combustion synthesis technique,<sup>16</sup> and solder alloys made by induction heating of the elemental metals in a variety of academic and commercial laboratories. Surface analytical techniques are required to observe the segregated impurity layer, which is typically too thin ( $< 1000 \text{ \AA}$ ) to observe with standard SEM/EDX techniques, where the sampling volume is on the order of  $2\text{--}3 \text{ }\mu\text{m}$  beneath the surface when using conventional accelerating voltages ( $\sim 20 \text{ kV}$ ) employed by most investigators doing EDX analysis.

A second solution is to devise a method to remove the alloy impurities after they have segregated. A method<sup>16</sup> to exploit, rather than mitigate, the effects of impurity surface segregation is by reheating the synthesized alloys, which enables segregation to occur, and then skimming or cleaning off the impurity shell. As shown above, for many alloys, the interiors of poorly wetted droplets of alloy are pure to the detection limit of Auger and EDX spectroscopy. In this way, segregation works as a method for producing ultrapure alloys.

A third solution is to introduce materials into the contact system, which possess a high chemical affinity for the segregating impurities. The materials can be introduced either as a surface coating or by incorporation into the alloy during synthesis and act to suppress segregation by tying up the alloy impurities during compound formation. This is one of the purposes of flux used in solder pastes. When flux is prohibited, reactive elements can be employed. We have used this method successfully to purify liquid boride and arsenide alloys used for high-brightness liquid metal ion sources by introducing boron into the contact system, which ties up the segregated carbon during formation of boron carbide.<sup>17</sup>

Electronics assembly process engineers who deal with solderability, adhesion, and assembly issues should be aware that segregated impurities may be the root cause of poor wetting and adhesion. Given the widespread appearance of impurity blocking layers, it is fortuitous that modern solder alloys exhibit a high joint reliability. The reason is twofold. In many highly reactive wetting systems, such as the wetting of solder alloys to Ni–Au, the high rate of Au dissolution and chemical reaction with the substrate is sufficient to overcome the blocking effect of segregated carbon, which is often found to reside on the alloy surface as a cracked inert mass of material (cf. Fig. 9). Second, contemporary solder pastes contain powerful fluxes, which clean the contacting surfaces of carbon as well as oxygen and other surface impurities. We know this is true due to wetting studies in our laboratory<sup>18</sup> involving organic solder preservative (OSP). Most solder pastes wet board finished of OSP, which consists of a thin film of protective organic (carbon) over Cu which protects the Cu from oxidation and then volatilizes during reflow.

There are several driving factors for surface segregation; in fact, Gibbs<sup>19</sup> developed a comprehensive thermodynamic formalism for surface segregation over a century ago. Experimental verification of the Gibbs theory awaited the development of surface spectroscopy in the 1970s. Most experimental studies of surface segregation using AES have been for the case of solid binary metal alloys. In their 1979 paper, Wynblatt and Ku<sup>20</sup> report that surface segregation experiments had been done on a dozen or so binary alloy systems at that time. Impurity segregation, where C, O, Ca, S, and other nonmetals repeatedly appeared on the surfaces of the alloys, was considered to be a nuisance in the early experiments, whose goal was to examine monolayer-scale segregation. Removal of these strongly segregating contaminants (usually by repeated sputter/heating cycles or reaction with oxygen) was important before starting the “true” segregation experiment involving the binary alloy components. This was because the impurities could interact preferentially with one or the other of the binary alloy elements and either enhance or suppress the natural segregating tendency of the uncontaminated alloy. Wynblatt and Ku<sup>21</sup> remark that “these species arise from strongly segregating tramp impurities present in the bulk alloy in trace quantities, and they can sometimes prove very difficult to remove.”

The complex nature of multicomponent solder alloys pose a challenge for the theories of surface segregation, most of which are based on ideal solutions having ideal surfaces at equilibrium. The simplest monolayer ideal-solution model<sup>22</sup> of surface segregation shows that low surface tension elements are likely to surface segregate, while the more realistic approach of Lea and Seah,<sup>23</sup> who developed a model for surface segregation based on the diffusion equation, shows that impurity segregating species should increase with temperature. Owing in part to the difficulties in measuring accurate surface tension values, standard compilations of surface tension are lacking or inadequate; for metals, however, there is an excellent correlation between surface tension and the heat of sublimation  $\Delta H_{\text{subl}}$ , because both

properties are related to creation of a unit area of surface. For semiconductors, semimetals, and insulators, most tabulated values in the literature show that the elements of lowest surface tension are the nonmetals (e.g., C, N, O, F, P, Cl, and S). Nonmetallic elements are frequently dubbed surface-active since they are the elements commonly observed on “clean” (99.999% pure) metal surfaces by surface analytical techniques. Figures 6–9 show several of these nonmetals appearing on the surfaces of heated mixed formulation, SAC, and Sn-37Pb alloys. Bulk contaminants, which are pinned in solid metal alloys at the grain boundaries, are released at melting when the boundaries disappear and surface segregate in order to minimize the overall free energy of the system.

## V. CONCLUSIONS

- (1) Wetting of mixed formulation series solder alloys is directly influenced by surface segregation of low-level bulk alloy impurities.
- (2) The major segregating impurities are C and O at the molten solder alloy surface.
- (3) The impurity segregation is not temperature reversible.
- (4) The impurities form a high surface tension shell around the alloy, which inhibits chemical reaction with the substrate, required for good wetting.
- (5) The interior of poorly wetted droplets of alloy is composed of pure alloy material, which allows for varying amounts of good wetting and spreading depending on the contacting materials. Wetting is sluggish where the carbon shell remnant is located.
- (6) Impurity surface segregation has been observed over a wide range of alloys synthesized by a variety of different alloy manufacturing techniques.
- (7) Solder fluxing remedies the problem with impurity segregation by cleaning both carbon and oxygen from surfaces.
- (8) The existence of surface segregation in molten liquids calls into question many previous studies of wetting that were conducted blind without the advantage of surface analytical tools such as Auger spectroscopy.

## ACKNOWLEDGMENTS

The authors gratefully acknowledge the industrial members of the Center for Advanced Vehicle Electronics and Extreme Environment Electronics (CAVE3) for continued support of this work.

<sup>1</sup>S. Hardy and J. Fine, in *Materials Processing in the Reduced Gravity Environment of Space*, edited by G. E. Rindone (Elsevier, Amsterdam, 1982), p. 503.

<sup>2</sup>S. Berglund and G. A. Somorjai, *J. Chem. Phys.* **59**, 5537 (1973).

<sup>3</sup>L. Goumiri and J. C. Joud, *Acta Metall.* **30**, 1397 (1982).

<sup>4</sup>F. Hua, R. Aspandiar, G. Clemons, and C. K. Chung, *Proceedings of the SMTA International Conference* (2005), pp. 246–252.

<sup>5</sup>A. R. Zbrzezny, P. Snugovsky, T. Lindsay, and R. Lau, *IEEE Trans. Electron. Packag. Manuf.* **29**, 211 (2006).

<sup>6</sup>B. Nandagopal, *Proceedings of the SMTA International Conference* (2005), pp. 861–870.



- <sup>7</sup>J. Nguyen and D. Shangguan, *Proceedings of the 57th Electronic Components and Technology Conference* (2007), pp. 1340–1349.
- <sup>8</sup>C. K. Chung, R. Aspandiar, K. F. Leong, and C. S. Tay, *Proceedings of the 52nd Electronic Components and Technology Conference* (2002), pp. 168–175.
- <sup>9</sup>C. E. Wicks and F. E. Block, *Thermodynamic Properties of 65 Elements—Their Oxides, Halides, Carbides, and Nitrides*, Bureau of Mines Bulletin 605 (U.S. Government Printing Office, Washington, DC, 1963).
- <sup>10</sup>A. Savitzky and M. Golay, *Anal. Chem.* **36**, 1627 (1964).
- <sup>11</sup>P. W. Palmberg, G. E. Riach, R. E. Weber, and N. C. MacDonald, *Handbook of Auger Electron Spectroscopy* (Physical Electronics Industries, Edina, MN, 1972).
- <sup>12</sup>M. J. Bozack, J. C. Suhling, Y. Zhang, Z. Cai, and P. Lall (submitted).
- <sup>13</sup>NIST Material Measurement Laboratory, [http://www.metallurgy.nist.gov/solder/clech/Sn-Ag-Cu\\_Other.htm#Young](http://www.metallurgy.nist.gov/solder/clech/Sn-Ag-Cu_Other.htm#Young).
- <sup>14</sup>M. J. Bozack, L. W. Swanson, and A. E. Bell, *J. Mater. Sci.* **22**, 2421 (1987).
- <sup>15</sup>P. Kuisma-Kursula, *X-Ray Spectrom.* **29**, 111 (2000).
- <sup>16</sup>M. J. Bozack and P. R. Davis, *Mater. Sci. Eng., A* **150**, 255 (1992).
- <sup>17</sup>M. J. Bozack, A. E. Bell, and L. W. Swanson, *J. Phys. Chem.* **92**, 3925 (1988).
- <sup>18</sup>M. J. Bozack, J. C. Suhling, Y. Zhang, Z. Cai, and P. Lall (submitted).
- <sup>19</sup>J. W. Gibbs, *The Scientific Papers of J. Willard Gibbs* (Dover, New York, 1961), Vol. **1**, p. 219.
- <sup>20</sup>P. Wynblatt and R. C. Ku, in *Interfacial Segregation*, edited by W. C. Johnson and J. M. Blakely (American Society for Metals, Metals Park, OH, 1979), p. 127.
- <sup>21</sup>P. Wynblatt and R. C. Ku, in *Interfacial Segregation*, edited by W. C. Johnson and J. M. Blakely (American Society for Metals, Metals Park, OH, 1979), p. 117.
- <sup>22</sup>G. A. Somorjai, *Introduction to Surface Chemistry and Catalysis* (John Wiley & Sons, New York, 1994), p. 285ff.
- <sup>23</sup>C. Lea and M. P. Seah, *Philos. Mag.* **35**, 213 (1977).